NASA TECHNICAL MEMORANDUM

NASA TM X-2819

NASA TM X-2819

COMPARISON OF TEMPERATURE DATA FROM AN ENGINE INVESTIGATION FOR FILM-COOLED AND NON-FILM-COOLED, SPANWISE-FINNED VANES INCORPORATING IMPINGEMENT COOLING

by Daniel J. Gauntner

Lewis Research Center
Cleveland, Ohio 44135

NATIONAL AERONAUTICS AND SPACE ADMINISTRATION • WASHINGTON, D. C. • JULY 1973

1. Report No.	2. Government Accession No.	3. Recipient's Catalog No.
NASA TM X-2819		

4. Title and Subtitle	5. Report Date
COMPARISON OF TEMPERATURE DATA FROM AN ENGINE INVESTIGATION FOR FILM-COOLED AND NON-FILM-COOLED, SPANWISE-FINNED VANES INCORPORATING IMPINGEMENT COOLING	July 1973
	6. Performing Organization Code
7. Author(s)	8. Performing Organization Report No.
Daniel J. Gauntner	E-7386
	10. Work Unit No.
9. Performing Organization Name and Address	501-24
Lewis Research Center National Aeronautics and Space Administration Cleveland, Ohio 44135	11. Contract or Grant No.
	13. Type of Report and Period Covered
12. Sponsoring Agency Name and Address	Technical Memorandum
National Aeronautics and Space Administration Washington, D.C. 20546	14. Sponsoring Agency Code

15. Supplementary Notes

16. Abstract

The experimental temperature characteristics of two spanwise-finned, impingement-cooled vanes, one with film cooling and one without film cooling, were investigated in a modified J-75 research turbojet engine. Values of maximum temperature, average temperature, and maximum chordwise temperature difference were compared for the two vanes at the midspan. An analytical redesign of the two vane configurations indicated that the maximum and average temperatures and the maximum chordwise temperature difference could be significantly lowered. The experimental tests indicated that suction-surface film cooling may cause increased heat transfer near the trailing edge of the vane.

17. Key Words (Suggested by Author(s))	18. Distribution Statement
Turbine cooling Air-cooled vane Film cooling Suction-surface film cooling	Unclassified - unlimited

19. Security Classif. (of this report)	20. Security Classif. (of this page)	21. No. of Pages	22. Price*
Unclassified	Unclassified	27	$3.00

* For sale by the National Technical Information Service, Springfield, Virginia 22151

COMPARISON OF TEMPERATURE DATA FROM AN ENGINE INVESTIGATION FOR FILM-COOLED AND NON-FILM-COOLED, SPANWISE-FINNED VANES INCORPORATING IMPINGEMENT COOLING

by Daniel J. Gauntner

Lewis Research Center

SUMMARY

A comparison was made of the experimental temperature characteristics of two spanwise finned, impingement cooled vanes, one with film cooling and one without film cooling, in a modified J-75 research turbojet engine. Experimental data were taken for gas temperatures ranging from 1366 to 1644 K (2000° to 2500° F), gas pressures from 20.7 to 28.3 newtons per square centimeter absolute (30 to 41 psia), inlet cooling-air temperatures from 297 to 811 K (75° to 1000° F), and coolant- to gas-flow ratios from 0.02 to 0.12. The local vane midspan temperature data were correlated for a wide range of operating conditions by a temperature-difference ratio (gas temperature minus vane temperature divided by gas temperature minus coolant-inlet temperature) plotted against the local coolant- to gas-flow ratio.

The experimental data were used as a base to calculate improvements in the vane temperature characteristics. These possible improvements resulted from an analytical redesign of the coolant flow distribution and the vane internal geometry. The redesign technique produced analytical values of maximum vane temperatures, average vane temperatures, and maximum vane chordwise temperature differences which were lower than the corresponding values obtained from the experimental data by as much as 69 K (125° F), 25 K (45° F), and 57 K (103° F), respectively.

The local temperature-difference ratios from the film-cooled and non-film-cooled vanes were used to determine the merits of the film-cooling configuration incorporated in the film-cooled vane. The experimental data indicated that film cooling may cause increased heat transfer near the trailing edge of the suction surface of the vane.

INTRODUCTION

The experimental heat-transfer characteristics of two air-cooled turbine vanes were investigated in a modified turbojet engine, and the improvements that could be expected by an analytical redesign were determined.

Materials currently in use for the fabrication of turbine vanes and blades are being pushed to the limit of their structural capabilities. High-performance engines of the future will operate at increased turbine-inlet temperatures. Thus, much attention has been devoted to the problem of cooling turbine vanes and blades. References 1 to 3 discuss experimental results for three vane configurations utilizing impingement, film, and convection cooling. In addition, references 1 and 2 also present analytical methods for improving the cooling performance of these vanes. The methods were based on a temperature-difference-ratio correlation derived from a one-dimensional heat balance. The complete derivation of the correlation method is given in reference 3.

The NASA Lewis Research Center is currently conducting a continuing program to investigate the cooling performance of vanes and blades for turbojet engines at turbine-inlet temperatures up to 1644 K (2500° F). The purpose of these investigations is to establish cooling designs for turbine vanes and blades which will perform reliably at 1644 K (2500° F).

The two vane configurations of the present investigation incorporated impingement-cooled leading edges, convection-cooled spanwise-finned midchord regions, and convection-cooled split trailing edges. The major difference between the two configurations was that one incorporated film cooling of the pressure and suction surfaces with a row of slots located approximately 2.54 centimeters (1.0 in.) from the stagnation line.

The experimental heat-transfer data reported herein were obtained at sea-level conditions with the use of a special research turbojet engine capable of being operated at turbine-inlet temperatures to 1644 K (2500° F). The tests were conducted for turbine-inlet temperatures that ranged from 1366 to 1644 K (2000° to 2500° F), gas pressures from 20.7 to 28.3 newtons per square centimeter absolute (30 to 41 psia), cooling-air temperatures from 297 to 811 K (75° to 1000° F), and coolant- to gas-flow ratios of 0.02 to 0.12.

APPARATUS

Engine

The research engine incorporated a modified version of the high-pressure spool, combustor, and turbine assembly of a J-75 turbojet engine. The engine was capable of being operated at turbine-inlet gas temperatures up to 1644 K (2500° F). One feature of

the engine was the use of separate cooling-air systems for the turbine components. The positioning of the five test vanes in the turbine assembly is shown in reference 1. These vanes were provided coolant from a laboratory air source that was completely independent of the air source used to cool the remaining 67 vanes in the turbine. The engine and test cell are completely described in reference 4.

Test Vanes

Two basic configurations of test vanes were investigated. One configuration used film cooling and is hereinafter referred to as "vane A." The other vane configuration had no film-cooling provisions and is referred to as "vane B."

Vane A. - A photograph of vane A is shown in figure 1(a), and a typical cross section of the vane is shown in figure 1(b). The vane span was 10.2 centimeters (4 in.), and the midspan chord length was 6.4 centimeters (2.5 in.). Cooling air entered the vane through the cooling-air inlet tube located on the vane tip platform. From a plenum chamber contained within the tip platform, the air was distributed into a leading-edge insert plenum and into nine midchord spanwise passages. The air which entered the leading-edge plenum flowed spanwise and exited in a chordwise direction through a row of 46 equally spaced impingement holes. These holes were 0.127 centimeter (0.05 in.) in diameter, spaced 0.2 centimeter (0.08 in.) apart, and located 0.53 centimeter (0.210 in.) from the inside surface of the leading edge of the vane. On a dimensionless basis, the z/d was 4.2, and c/d was 1.6. (All symbols are defined in the appendix.) The air then divided to flow through 65 equally spaced chordwise passages along each of the inside suction and pressure surfaces. The passages started at nominally 1.8 centimeters (0.72 in.) from the stagnation point. The passages were formed by fins which were integral with the vane wall and which augmented the heat-transfer area. The passages were 0.114 centimeter (0.045 in.) high and 0.112 centimeter (0.044 in.) wide. The fins were nominally 0.036 centimeter (0.014 in.) thick. The passages were capped by the boundary wall of the leading-edge insert plenum.

The cooling air then exited the vane through single rows of interrupted film-cooling slots on both sides of the vane. The suction-surface slots were 2.72 centimeters (1.07 in.) from the outside leading edge of the vane, and the pressure surface slots were 2.2 centimeters (0.88 in.) from the outside leading edge. The suction-surface slots were angled nominally 27° from the vane surface, while the pressure-surface slots were angled nominally 30° from the vane surface, as shown in figure 1(b). The suction surface contained ten identical spanwise slots, each 0.394 centimeter (0.155 in.) by 0.056 centimeter (0.022 in.). The pressure-surface slots consisted of a linear array of three different spanwise slot groups. The vane tip group had five spanwise passages, each 0.427 centimeter (0.168 in.) by 0.094 centimeter (0.037 in.); the midspan group had five

spanwise passages, each 0.427 centimeter (0.168 in.) by 0.061 centimeter (0.024 in.); and the hub group had five spanwise passages, each 0.437 centimeter (0.172 in.) by 0.056 centimeter (0.022 in.).

The inlet cooling air which entered the nine midchord spanwise passages flowed radially inward adjacent to the suction and pressure surfaces to the hub of the vane. At the hub, the air from the suction and pressure surfaces recombined in the midchord plenum and flowed radially outward toward the vane tip. The midchord plenum was open at the trailing edge (see fig. 1(b)), thus allowing the cooling air to flow chordwise, outward through 13 passages in the split trailing edge of the vane, and out into the gas stream. Table I shows the dimensions of the midchord spanwise passages, which are numbered in figure 1(b). The passages were formed in the vane wall by spanwise fins integral with the wall. The fins were 0.140 centimeter (0.055 in.) high, and 0.051 centimeter (0.020 in.) thick. The midchord passages were capped by the boundary wall of the midchord plenum. The passages in the split trailing edge were 0.076 centimeter (0.030 in.) high and 0.577 centimeter (0.227 in.) in the spanwise direction. The passages were formed by 12 chordwise fins, each 0.183 centimeter (0.072 in.) thick.

Vane B. - A photograph of vane B is shown in figure 1(a), and a typical cross section is shown in figure 1(c). Vane B was similar to vane A except that it had no provision for film cooling. In vane B, the air which in vane A would exit through the film-cooling slots entered, instead, the midchord plenum after flowing through 65 equally spaced chordwise passages. In addition, there were 49 leading-edge impingement holes, each 0.084 centimeter (0.033 in.) in diameter, located 0.53 centimeter (0.21 in.) from the inside surface of the leading edge, and spaced every 0.196 centimeter (0.077 in.). The z/d was 6.4, and the c/d was 2.33. Also, the passage height in the split trailing edge was larger, being 0.119 centimeter (0.047 in.). The larger flow area in the trailing edge of vane B was needed because all of the coolant flow left the vane through its trailing edge.

INSTRUMENTATION

Engine

The research engine was instrumented extensively to provide information on the general operating conditions of the engine and also to provide detailed information relative to the environmental conditions in the turbine test section. Eight remotely actuated water-cooled temperature probes were used to determine the composite turbine inlet temperature profile. One of these probes was located behind each combustor. Each probe was traversed in a radial direction and was programmed to stop automatically at

nine equally spaced locations. The eight circumferential probe positions and nine radial stops of each probe provided 72 different points of temperature measurement for the composite profile. The details of the instrumentation in the combustion air, fuel, and cooling-air systems are given in reference 4.

Test Vanes

Thermocouples. - Vane A and Vane B were each instrumented in the following manner. Five test vanes were instrumented with a total of 25 Chromel-Alumel thermocouples embedded in the walls of the airfoils. Three of the five test vanes contained 23 of the 25 thermocouples, however, and only these 23 midspan thermocouples are presented herein. Because of structural considerations, the thermocouples were distributed 8, 8, and 7 among the three vanes. A composite vane thermocouple layout is presented in figure 1(b) for vane A and in figure 1(c) for vane B. Also, the vane-surface locations of the thermocouples are presented, in dimensionless form, in table II.

The cooling air temperature at the inlet to each of the individual vanes was determined from a single Chromel-Alumel thermocouple installed upstream of the entrance to the cooling air inlet tube.

Pressure taps. - A single wall static pressure was used to indicate the cooling air pressure at the inlet to an individual vane. The wall static tap was located in a straight section of a cooling air inlet pipe that was an upstream extension of the cooling air inlet tube.

TEST PROCEDURE

The five thermocoupled test vanes were installed adjacent to each other in the turbine stator assembly. The engine was operated over a range of turbine inlet temperatures from 1366 to 1644 K (2000° to 2500° F) and turbine inlet pressures from 20.7 to 28.3 newtons per square centimeter (30 to 41 psia). The tests were made with the cooling-air temperature at the vane inlet at values ranging from 297 to 811 K (75° to 1000° F). The compressor pressure ratio had a value of approximately 3 with the engine inlet exposed to atmospheric pressure.

The test-vane coolant flows were reduced stepwise for each series of runs until a maximum vane metal temperature of about 1278 K (1840° F) was reached; this is considered the maximum safe operating temperature for the vane configuration. After the minimum coolant flow condition was reached, a few additional runs at increased coolant flow were made to serve as checkpoints for the data taken previously. This general

procedure was usually repeated for each series of runs. The test-vane coolant flow ratios ranged from about 0.02 to 0.12.

ANALYSIS METHODS

Temperature-Difference-Ratio Correlation

Local temperature data taken in heat-transfer tests can be used to compare different turbine vane designs. The simplest method of using the temperature data is to correlate them with the local coolant- to gas-flow ratio. The investigations of reference 3 presented a method of correlation which represented the average temperature data to within 5 percent. The local temperature data were correlated with a maximum deviation of 16 percent.

The method of correlation started with a one-dimensional heat balance given by equation (1).

$$h_g S_g (T_{ge} - T_{wo}) = h_c S_c (T_{wi} - T_c) \tag{1}$$

For the gas temperature and pressure levels reported herein, the following approximate and simplifying equivalences are stated:

$$T_{wo} = T_{wi} = T_w$$

$$T_c = T_{ci}$$

$$T_{ge} = T_{ti}$$

Then, if the exponents of the Reynolds numbers in expressions for h_g and h_c are assumed equal, the following correlation equation results:

$$\varphi = \frac{1}{1 + C_1 \left(\frac{\dot{w}_c}{\dot{w}_g} \right)^{C_2}} \tag{2}$$

where

$$\varphi = \frac{T_{ti} - T_w}{T_{ti} - T_{ci}} \tag{3}$$

Wall temperature distributions can be obtained by combining equations (2) and (3) to give equation (4).

$$T_w = T_{ti} - \frac{T_{ti} - T_{ci}}{1 + C_1\left(\frac{\dot{w}_c}{\dot{w}_g}\right)^{C_2}} \tag{4}$$

In equation (2), the constants C_1 and C_2 can be found from a least-squares fit of the data in the form $(1 - \varphi)/\varphi$ as a function of $\dot{w}_c/\dot{w}_g$. Further details of the derivation are given in reference 3.

Vane Temperature Characteristics

While knowledge of the temperature distribution is important, another important element in a vane design is the vane life. The steady-state lives of turbine vanes depend, in part, on average temperatures, maximum temperatures, and maximum temperature differences over the vane surface. These temperature characteristics for vanes A and B can be easily found by using equation (4). The comparison of the characteristics of vanes A and B are made with identical values of T_{ti}, T_{ci}, and $\dot{w}_c/\dot{w}_g$.

Redesign Techniques

Theoretical improvements in vane temperature characteristics can be made by making a paper redesign of vanes A and B according to the following techniques. The improvements are realized by a more efficient distribution of the coolant flow and by the use of vane interior cooling geometries which produce optimum modes of impingement and convective heat transfer.

Redistribution of coolant flow. - In order to evaluate experimental heat-transfer data for vanes having different cooling configurations, it is necessary to know the coolant distribution inside of the vanes. Reference 1 describes a bench-test method of obtaining local coolant flow distributions.

When the flow distribution is known for a vane configuration for which experimental temperature data exist, it may be possible to improve the temperature characteristics of

a vane by redistributing the coolant flow. The redistribution is accomplished by varying the minimum area restrictions in the leading-edge (the row of impingement holes) and in the trailing-edge regions of the vane (the passages in the split trailing edge, as shown in fig. 1). Thus, the flow and the area change in such a way that $\dot{w}/A_{min}$, where A_{min} is the minimum area restriction, remains constant. The Reynolds number does not remain constant at the points of minimum area, since the hydraulic diameter changes. A correction factor for the change in the hydraulic diameter is used in the vane redesign analysis.

Impingement heat transfer. - One of the primary objectives of early impingement heat-transfer studies was the establishment of the nozzle-to-nozzle and nozzle-to-plate spacings which produced the optimum heat transfer. Reference 5 found the maximum heat transfer at the stagnation point of a flat plate to occur at a z/d value between 6 and 7 for a single circular jet. For a square array of jets impinging on a flat plate, correlation of data within 10 percent was achieved for z/d values between 2 and 8. Reference 6 found almost no change in heat-transfer coefficients when the value of z/d was less than 6 for a single jet impinging on a flat plate. The optimum spacing for multiple arrays of jets was found to occur at z/d values between 2 and 4. Vanes A and B were designed based on the results of reference 5 and had z/d values of 4.2 and 6.4, respectively. Since the time of the vane designs, much work has been done on impingement heat transfer from concave cylindrical surfaces. Reference 7 concludes that for a z/d value of 1, heat-transfer rates are no less than 90 percent of the maximum for all conditions of c/d and l/b_{es}. Thus, vanes A and B can be redesigned according to the results of reference 7 to improve the impingement heat transfer.

Use of vane-temperature-difference correlations. - The correlation of experimental data (eq. (2)) can be used to make analytical improvements in the vane temperature distributions. The following expressions for the redesign analytical temperature distribution (eq. (5)) and the allowable hotspot turbine inlet temperature (eq. (6)) were derived in reference 2:

$$T_w = T_{ti} - \frac{(T_{ti} - T_{ci})}{1 + \frac{h_{c,o}}{h_{c,r}} \left[C_1 \left(\frac{\dot{w}_c}{\dot{w}_g} \right)^{C_2} \right]_o} \tag{5}$$

$$T_{ti} = T_w + \frac{T_w - T_{ci}}{\frac{h_{c,o}}{h_{c,r}} \left[C_1 \left(\frac{\dot{w}_c}{\dot{w}_g} \right)^{C_2} \right]_o} \tag{6}$$

Note that C_1 and C_2 are the original constants listed in table III; $\dot{w}_c/\dot{w}_g$ is the redesign local coolant flow. At thermocouple positions where only $\dot{w}_c/\dot{w}_g$ changes, the value of $h_{c,o}/h_{c,r}$ is 1. At other thermocouple positions, $h_{c,o}/h_{c,r}$ also incorporates corrections for changes in impingement geometry, hydraulic diameter, and/or fin efficiencies, as discussed in references 2 and 3. The T_w in equation (6) is the maximum allowable vane wall temperature. Note that equation (6) is for a redesign hotspot temperature. If an original hotspot temperature is wanted, $h_{c,o}/h_{c,r}$ is set equal to 1.0.

Comparison of Local Temperature Difference Ratios

Because of the similarity between vanes A and B in their midchord and trailing-edge regions, a comparison of local temperature difference ratios can show the merits of film cooling in an engine environment. The use of equation (1), with T_{aw} in place of T_{ge}, in conjunction with equation (3) and the definition of the film effectiveness, η_f, yields the following expression describing the heat transfer for a segment of convection- and film-cooled wall:

$$\frac{1 - \varphi}{\varphi} = \frac{h_g S_g}{h_c S_c}\left[1 - \frac{\eta_f}{\varphi}\left(\frac{T_{ti} - T_{cs}}{T_{ti} - T_c}\right)\right] \tag{7}$$

If equation (7) is solved for φ (renamed φ_f) and divided by the expression for φ when no film cooling is present (i.e., $\eta_f = 0$ in eq. (7)), an expression results which shows the relative merits of film cooling compared with no film cooling.

$$\frac{\varphi_f}{\varphi} = \frac{1 + \lambda}{1 + \lambda_f}\left[1 + \lambda_f \eta_f \left(\frac{T_{ti} - T_{cs}}{T_{ti} - T_c}\right)\right] \tag{8}$$

where $\lambda = h_g S_g / h_c S_c$ and $\lambda_f = h_{g,f} S_g / h_{c,f} S_c$. For the following analysis, S_g is assumed to equal S_c, and $h_{c,f}$ equals h_c.

If $h_{g,f}$ is equal to or less than h_g (i.e., $\lambda_f \leq \lambda$), it is obvious from equation (8) that φ_f will be greater than φ for all values of η_f greater than zero. On the other hand, if $h_{g,f}$ is greater than h_g, it is possible that φ_f can be less than φ, depending on the magnitude of η_f.

RESULTS AND DISCUSSION

Coolant Flow Distribution

The distribution of coolant flow inside vane A is shown in figure 2. The curves were found from static cold-flow bench tests for three values of total pressure taken according to the procedure discussed in reference 1. The percent of the total inlet coolant flow exiting from any vane region is shown to vary with the ratio of the coolant-inlet-static pressure to turbine-inlet-total pressure. The predominant feature of the curve is that below a pressure ratio of 0.96, hot gas will be drawn into the vane through the pressure-surface film-cooling slots. Since the value of the total-coolant to gas-flow ratio at which the pressure ratio equals 0.96 is also dependent on cooling air temperature, a working curve (not shown herein) of total-coolant to gas-flow ratio as a function of pressure ratio was made, with the experimental coolant temperature as a parameter. A curve of this type shows the total-coolant to gas flow rate, for each value of coolant temperature, at which hot gas will be circulating into the vane. Such curves for the data of vane A showed, for a coolant temperature of 311 K (100° F), the flow ratio to be 0.048. For an extrapolation to 922 K (1200° F), the flow ratio was found to be 0.036.

For vane B, the distribution of flow between the leading-edge passages and the midchord spanwise passages was found to be constant, with 41.5 percent passing through the leading edge and the remaining 58.5 percent of the total coolant flow passing through the spanwise passages. This constant distribution was expected, since the coolant flow in the passages reunites in the vane midchord plenum before exiting through the vane trailing edge. The flow split, then, is determined by the minimum areas in the leading-edge flow path and in the midchord spanwise passage flow path. The flow split was obtained experimentally by alternately blocking the impingement holes, and then the spanwise passages. The blockage of the impingement holes was achieved by placing a rubber shim in the leading-edge insert plenum (see fig. 1(c)) up against the line of impingement holes. This was done before the hub platform was attached. To block the spanwise passages, the tip platform was removed, a plate was placed over the passages, and the platform was replaced. The ambient cooling air flow rates thus obtained were then normalized.

Midspan Chordwise Temperature Distributions

All local experimental temperatures were correlated with the use of the temperature difference method discussed previously in the "ANALYSIS METHODS" section. The constants C_1 and C_2 required to determine the local temperatures in equation (4) are listed in table III for each local thermocouple location around the midspan vane periphery. The constants in table III were obtained by correlating the local temperature data with the

local flow rate for the entire range of variables covered during operation of the research engine.

Both the original and the redesign chordwise temperature distributions for the two vane configurations are shown in figure 3. The original distributions were obtained from the local correlated temperature data. The data in figure 3 were for a vane inlet cooling air temperature of 922 K (1200° F), a coolant- to gas-flow ratio of 0.05, and a turbine inlet temperature of 1528 K (2290° F). This value of the turbine inlet temperature was chosen because it was the value needed to maintain a maximum wall temperature equal to or less than 1278 K (1840° F) on the redesign vanes A and B, as discussed later, in the "Comparison of Original and Redesign Vane Characteristics" section. Using a single value for the turbine inlet temperature also allows comparison between the original vane and the redesign vane.

Comparison of the original temperature distributions shows, in general, that the two vane configurations cooled similarly in the leading-edge region, with the maximum leading-edge temperature being of the order of 1325 K (1925° F). The midchord regions of both vanes were considerably cooler than the leading-edge regions, with vane A being cooler than vane B, particularly downstream of the film-cooling slots. The trailing-edge temperatures were between those of the leading-edge and midchord regions. The maximum temperature difference between the leading edge region and the lowest midchord temperature was greater for the film-cooled vane than for the non-film-cooled vane.

Analytical Vane Redesign

The high leading-edge vane temperatures and the high temperature gradients between the leading-edge and the midchord regions of vanes A and B inspired analytical redesigns for the two vanes. The objectives were to lower the maximum vane temperatures and to decrease the temperature gradients. Both redesigns were performed for a turbine inlet temperature of 1528 K (2290° F), an inlet coolant temperature of 922 K (1200° F), and a total coolant- to gas-flow ratio of 0.05.

Vane A. - The analytical redesign of vane A was accomplished by redistributing the coolant flow, by moving the row of leading-edge impingement holes closer to the inside surface of the vane, by extending the chordwise fin surfaces on the pressure-side leading-edge region, and by changing the geometry of the chordwise fins on the pressure surface and in the trailing edge to improve the fin efficiencies.

The original temperature distribution for vane A was compared with the distribution that resulted when the vane was analytically redesigned to operate at a coolant- to gas-flow ratio of 0.05, a coolant inlet temperature of 922 K (1200° F), and a p_{ci}/P_{ti} of 1.0. This value of p_{ci}/P_{ti} is in the range of a normal engine operating conditions.

Using the methods of reference 1 yielded the revised flow distribution of 55.4 percent of the total coolant flow leaving the trailing-edge exits, 31.4 percent leaving the suction-surface exits, and 13.2 percent leaving the pressure-surface exits. With this information and equation (5), the analytical temperature distribution that would result for the redesign vane A was calculated. Characteristics of the original and redesign distributions are discussed in the "Comparison of Original and Redesign Vane Characteristics" section.

Vane B. - The redesign of vane B followed the same methods used for vane A, except that there were no chordwise fin extensions placed in the leading edge. The flow distribution was adjusted to 57 percent from 41.5 percent (of the total coolant flow) through the impingement holes and to 43 percent from 58.5 percent (of the total coolant flow) through the spanwise passages.

The redesign vane B temperature distribution was obtained in the same manner and for the same gas and coolant conditions as discussed for vane A. The characteristics of these curves are discussed in the following section.

Comparison of Original and Redesign Vane Characteristics

The original and redesign vane temperature distributions are shown in figures 3(a) and (b) for vanes A and B, respectively. The analytical redesign distributions for vanes A and B show that leading-edge temperatures have been reduced with respect to the original experimental distributions. The redesign leading-edge temperatures are now at the same level as the redesign trailing-edge temperatures. Also, the temperature gradients between the leading edge and the midchord region have been reduced for both vanes.

The vane temperature characteristics for the vane A and B temperature distributions are listed in table IV. These characteristics include values of the maximum vane temperature, the maximum vane temperature difference, and the average vane temperature for both the original and the redesign vanes. The value of the hotspot turbine-inlet temperature used in the calculations was determined as follows. Since 1278 K (1840° F) is considered to be the maximum temperature the vane material can withstand, this wall temperature was used in equation (6) to calculate the hotspot turbine-inlet temperature for the redesign vanes A and B. The lower of the two values of hotspot turbine-inlet temperature was then used so that all comparisons of vane characteristics would be on the same gas-temperature basis. This lower temperature was calculated to be 1528 K (2290° F) for vane B, while the higher temperature was calculated to be 1565 K (2358° F) for vane A. If the maximum wall temperatures in the original designs of vanes A and B had been limited to 1278 K (1840° F), the hotspot turbine-inlet temperatures would have been only 1455 K (2160° F) and 1469 K (2185° F), respectively.

Some results can be drawn from the table. First, the vane design incorporating film cooling has a higher maximum vane temperature difference than does the vane design without film cooling. This result is expected, since film cooling will cool a local region of the wall to a temperature lower than might result with a similar vane design without film cooling, thus giving a larger maximum vane temperature difference. Second, the average vane temperature is not changed very much by the redesign techniques discussed herein when the gas temperature, coolant temperature, and coolant- to gas-flow ratio are held constant. And, third, when the hotspot turbine-inlet temperature is held constant for a given vane, there is a greater decrease in the maximum vane temperature (between the original and the redesigned vane) for the film-cooled vane than for the non-film-cooled vane. Or, with the maximum vane temperature, coolant temperature, and coolant- to gas-flow ratio all held constant, the redesign of a film-cooled vane will give a greater increase in hotspot turbine-inlet temperature than will a redesign of a non-film-cooled vane.

Table IV shows that the maximum vane temperature in the redesign case decreased 69 K (125° F) and 36 K (66° F) for vanes A and B, respectively. The maximum vane temperature difference for vane A decreased 57 K (103° F), while for vane B it decreased 55 K (98° F). The average temperature for vane A decreased 25 K (45° F), but the average temperature for vane B increased 5 K (9° F).

Comparison of Local Temperature Difference Ratios

The advantage of film cooling a local region of vane is shown qualitatively by equation (8), the ratio of the local temperature difference ratios for film-cooled and non-film-cooled vane designs. The equation shows that for the same vane geometry, the same inside coolant flow rate past the local region, and the same gas and coolant temperatures, φ_f should be greater than φ, for as far downstream from the point of injection as film cooling remains effective, if $h_{g,f}$ is equal to or less than h_g. Such a comparison of φ_f and φ is made for the experimental data of vanes A and B in figures 4(a) and (b) for thermocouples 8 and 1, respectively. For vane A, thermocouples 8 and 1 were approximately 3 and 75 slot widths, respectively, downstream of the film cooling slots.

Figure 4(a) shows vane A to be more effectively cooled than vane B, or φ_f is greater than φ. The comparison of the φ values of the intermediate thermocouples 7 to 3 on vanes A and B, although not presented, show the excess of the value of φ_f over φ to be less as the distance downstream of the film-cooling slots increases.

The comparison of local temperature difference ratios for thermocouple 1, shown in figure 4(b), exhibits an interesting phenomenon. For the same coolant and gas conditions, vane A is shown to be slightly more effectively cooled than vane B. However, although the flow is the same through the trailing edges of vanes A and B, the inside

Reynolds number (and thus h_c) is not, since the passage area in vane A is half the area of vane B. If the passage area of vane A is analytically made equal to that of vane B (thus equalizing the inside heat-transfer coefficients) and if variations in fluid properties are neglected, a modified local temperature difference ratio is obtained for vane A. The analytical adjustment of the passage area in vane A involved a hydraulic diameter correction to the φ expression, equation (2). This modification of the φ value of vane A is shown by the dashed curve in figure 4(b). This result appears to indicate that for the same gas, coolant, and geometrical conditions, film cooling is causing a detrimental effect on the cooling efficiency for the trailing-edge suction surface of vane A. The reason for this is not clearly understood, but it is possible that the suction-surface film cooling is tripping the boundary layer and causing turbulent flow. An analysis of equation (8) might explain the results of figure 4(b). If h_g is for laminar flow and $h_{g,f}$ is now for turbulent flow, λ_f would be greater than λ, and φ_f could be less than φ, even for cases where the film cooling is still active (i.e., $\eta_f > 0$).

A similar analysis was performed for the thermocouples downstream of the pressure surface slots. For each thermocouple, φ_f was greater than φ, showing film cooling to be effective over the entire pressure surface, where the boundary-layer flow is completely turbulent.

SUMMARY OF RESULTS

An experimental heat-transfer investigation of two spanwise - finned, impingement-cooled turbine vane configurations was made in a research-type turbojet engine. The following are the results of the investigation:

1. The experimental vane temperature data indicated that both vane configurations cooled similarly, with the midchord region of the film-cooled vane being somewhat cooler than that of the non-film-cooled vane. Both vane configurations exhibited relatively high leading-edge temperatures and large thermal gradients between the leading-edge and midchord regions.

2. The analytically redesigned film-cooled vane indicates that significant improvement of the cooling characteristics could be achieved by changes in the internal vane geometry (moving the leading-edge impingement holes closer to the inside surface, modifying the leading-edge and trailing-edge fin geometry, and reapportioning the coolant flow within the vane). These changes resulted in the following calculated temperature comparisons for a turbine inlet temperature of 1528 K (2290° F), a coolant temperature of 922 K (1200° F), and a coolant flow ratio of 0.05:

Film-cooled vane	Maximum vane temperature, K (^{O}F)	Average vane temperature, K (^{O}F)	Maximum chordwise temperature difference, K (^{O}F)
Redesigned	1257 (1803)	1210 (1718)	106 (191)
Original	1326 (1928)	1235 (1763)	163 (294)

3. The analytically redesigned non-film-cooled vane indicated that significant improvement of the cooling characteristics could be achieved by changes in the internal vane geometry, moving the leading-edge impingement holes closer to the inside surface, and reapportioning the coolant flow within the vane. These changes resulted in the following calculated temperature comparisons for a turbine-inlet temperature of 1528 K (2290^{O} F), a coolant temperature of 922 K (1200^{O} F), and a coolant flow ratio of 0.05:

Non-film-cooled vane	Maximum vane temperature, K (^{O}F)	Average vane temperature, K (^{O}F)	Maximum chordwise temperature difference, K (^{O}F)
Redesigned	1278 (1840)	1247 (1785)	74 (134)
Original	1314 (1906)	1242 (1776)	129 (232)

4. For a maximum allowable vane metal temperature of 1278 K (1840^{O} F), a cooling air inlet temperature of 922 K (1200^{O} F), and a coolant flow ratio of 0.05, the hotspot turbine-inlet temperature was found to be 1565 K (2358^{O} F) for the redesigned film-cooled vane. It was 1455 K (2160^{O} F) for the original design. For the redesigned non-film-cooled vane, the hotspot turbine-inlet temperature was 1528 K (2290^{O} F). It was 1469 K (2185^{O} F) for the original design.

5. When the correlated local metal temperature data were used to calculate local metal temperatures for equal vane operating conditions (turbine inlet temperature, cooling air temperature, coolant flow, and trailing-edge geometries) it was found that the temperature of the film-cooled vane near the trailing edge on the suction surface would be higher than that of the non-film-cooled vane. This indicates that film-cooling air

ejected from the front half of the vane may cause increased heat transfer on the trailing-edge suction surface.

Lewis Research Center,
National Aeronautics and Space Administration,
Cleveland, Ohio, April 12, 1973,
501-24.

APPENDIX - SYMBOLS

A	area for coolant flow in a vane region
b_{es}	equivalent slot width, $\pi d^2/4c$
C_1, C_2	constants in eq. (2)
c	center to center distance between impingement nozzles
d	nozzle diameter
h	heat transfer coefficient
L	surface length between leading edge and trailing edge
ℓ	surface length from stagnation point
P	total pressure
p	static pressure
S	heat transfer area
T	temperature
$\dot{w}$	flow rate
x	distance along surface from stagnation point or distance from film-cooling slot
z	distance from nozzle to impingement surface
η_f	film effectiveness, $\frac{T_{ge} - T_{aw}}{T_{ge} - T_{cs}}$
λ	$h_g S_g / h_c S_c$
φ	temperature difference ratio, $\frac{T_{ti} - T_w}{T_{ti} - T_{ci}}$

Subscripts:

aw	adiabatic wall
c	coolant
ci	coolant inlet
cs	coolant condition at the slot
f	film
g	gas

ge	effective gas
min	minimum
o	original design
r	redesign
ti	turbine inlet
w	wall
wi	inside wall
wo	outside wall
x	local flow

REFERENCES

1. Gauntner, James W.; Lane, Jan M.; Dengler, Robert P.; and Hickel, Robert O.: Experimental Heat Transfer and Flow Results of a Chordwise-Finned Turbine Vane With Impingement, Film, and Convection Cooling. NASA TM X-2472, 1972.

2. Yeh, Frederick, C.; Gladden, Herbert J.; and Gauntner, James W.: Comparison of Heat Transfer Characteristics of Three Cooling Configurations for Air-Cooled Turbine Vanes Tested in a Turbojet Engine. NASA TM X-2580, 1972.

3. Gladden, Herbert J.; Gauntner, Daniel J.; and Livingood, John N. B.: Analysis of Heat-Transfer Tests of an Impingement-Convection- and Film-Cooled Vane in a Cascade. NASA TM X-2376, 1971.

4. Calvert, Howard F.; Cochran, Reeves P.; Dengler, Robert P.; Hickel, Robert O.; and Norris, James W.: Turbine Cooling Research Facility. NASA TM X-1927, 1970.

5. Gardon, Robert; and Cobonpue, John: Heat Transfer Between a Flat Plate and Jets of Air Impinging on It. International Developments in Heat Transfer. ASME, 1963, pp. 454-460.

6. Huang, G. C.: Investigations of Heat-Transfer Coefficients for Air Flow Through Round Jets Impinging Normal to a Heat-Transfer Surface. J. Heat Transfer, vol. 85, no. 3, Aug. 1963, pp. 237-245.

7. Jenkins, C. W.; and Metzger, D. E.: Local Heat Transfer Characteristics of Concave Cylindrical Surfaces Cooled by Impinging Slot Jets and Lines of Circular Jets With Spacing Ratios 1.25 to 6.67. Tech. Rep. 694, Arizona State Univ., May 1969.

TABLE I. - DIMENSIONS OF MID-CHORD SPANWISE PASSAGES IN TEST VANES

Passage number (a)	Passage height, cm (in.)	Passage width, cm (in.)
1	0.140 (0.055)	0.368 (0.145)
2		0.401 (0.158)
3		0.360 (0.142)
4		0.360 (0.142)
5		0.351 (0.138)
6		0.277 (0.109)
7		0.648 (0.255)
8		0.577 (0.227)
9		0.648 (0.255)

[a]See fig. 1(b) for passage locations.

TABLE II. - DIMENSIONLESS SURFACE DISTANCES FOR THERMOCOUPLE LOCATIONS ON VANES A AND B

Suction surface		Pressure surface	
Thermocouple	Dimensionless surface distance, x/L (a)	Thermocouple	Dimensionless surface distance, x/L (b)
1	0.916	--	-----
2	.790	13	0.022
3	.671	14	.024
4	.605	15	.058
5	.554	16	.107
6	.496	17	.173
7	.434	18	.273
8	.381	19	.404
9	.264	20	.417
10	.147	21	.507
11	.096	22	.603
12	[c].079	23	.805

[a]Suction-surface L = 7.26 cm (2.86 in.).
[b]Pressure-surface L = 6.50 cm (2.56 in.).
[c]0.052 for vane B.

TABLE III. - VALUES OF CORRELATION-EQUATION (EQ. (2)) CONSTANTS C_1 AND C_2 FOR VANES A AND B

Thermocouple	Correlation-equation constants			
	C_1	C_2	C_1	C_2
	Vane A		Vane B	
1	0.102	-0.70	0.103	-0.72
2	.086	-.65	.131	-.65
3	.074	-.70	.077	-.69
4	.053	-.71	.072	-.67
5	.048	-.76	.066	-.71
6	.034	-.81	.086	-.65
7	.037	-.79	.084	-.65
8	.054	-.73	.106	-.65
9	-----	-----	.133	-.57
10	.032	-.79	.198	-.50
11	.024	-.90	.247	-.48
12	-----	-----	.241	-.48
13	.107	-.79	.454	-.32
14	.194	-.62	.480	-.35
15	.082	-.87	-----	-----
16	.192	-.43	.266	-.47
17	.255	-.34	.170	-.54
18	.212	-.33	.141	-.54
19	.0043	-1.43	.165	-.52
20	.0032	-1.51	.072	-.76
21	.0074	-1.29	-----	-----
22	.020	-1.06	.099	-.66
23	.023	-1.14	.154	-.71

TABLE IV. - SUMMARY OF VANE-TEMPERATURE CHARACTERISTICS

Temperature characteristics	Vane A		Vane B	
	Original	Redesign	Original	Redesign
Coolant to gas flow ratio	0.05	0.05	0.05	0.05
Coolant inlet temperature, K (^{O}F)	922 (1200)	922 (1200)	922 (1200)	922 (1200)
Maximum vane temperature, K (^{O}F)	1326 (1928)	1257 (1803)	1314 (1906)	1278 (1840)
Maximum vane temperature difference, K (^{O}F)	163 (294)	106 (191)	129 (232)	74 (134)
Average vane temperature, K (^{O}F)	1235 (1763)	1210 (1718)	1242 (1776)	1247 (1785)
Hotspot turbine-inlet temperature, K (^{O}F)	1528 (2290)	1528 (2290)	1528 (2290)	1528 (2290)

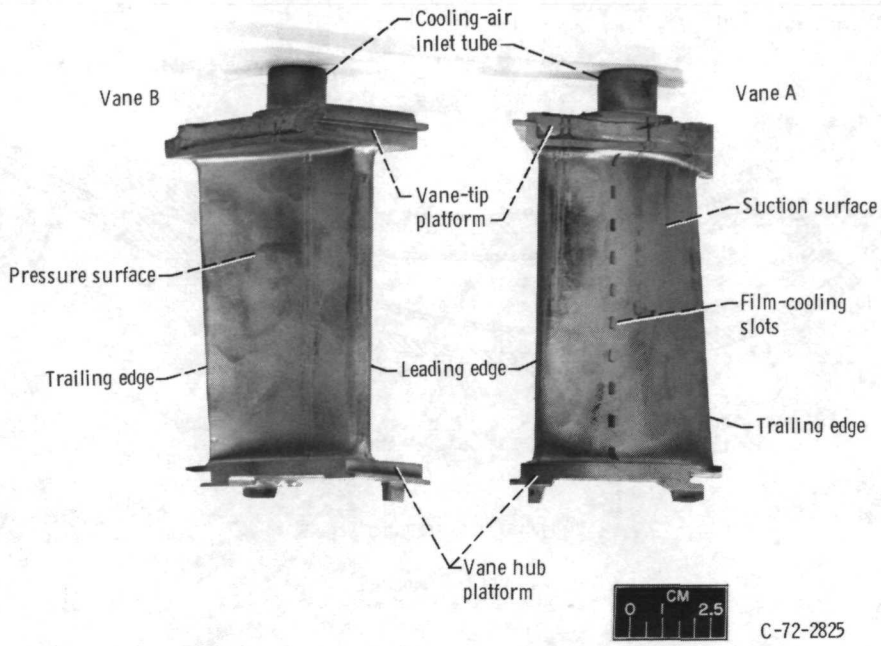

(a) Test-vanes.

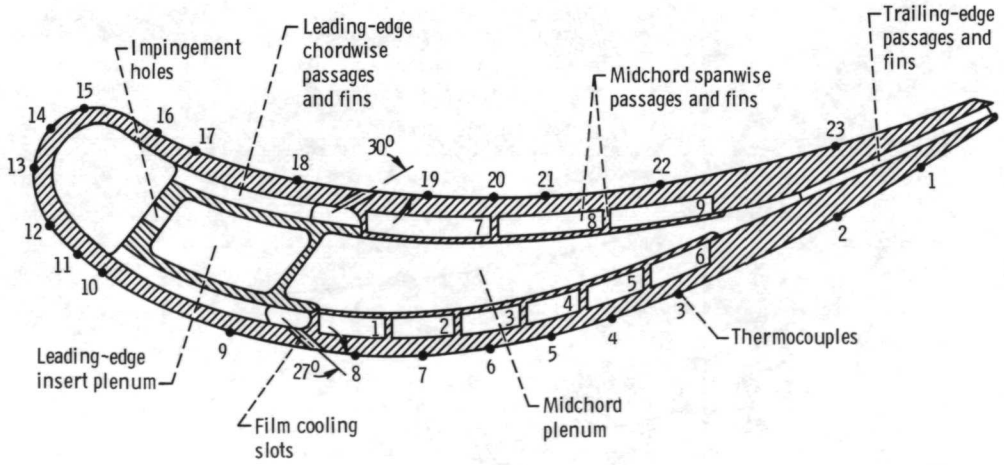

(b) Typical cross section of vane A.

Figure 1. - Test-vane assembly.

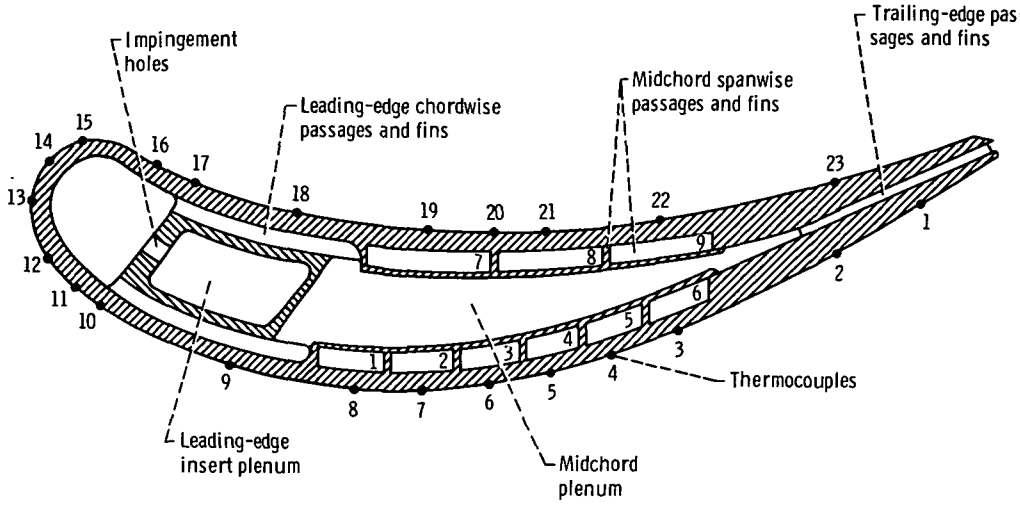

(c) Typical cross section of vane B.

Figure 1. - Concluded.

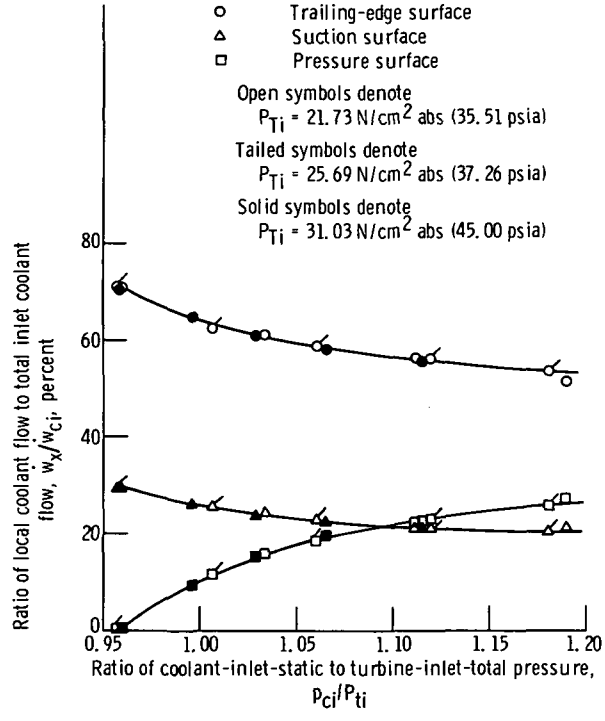

Figure 2. - Local coolant flow distribution as a function of the pressure ratio for vane A for ambient coolant temperature.

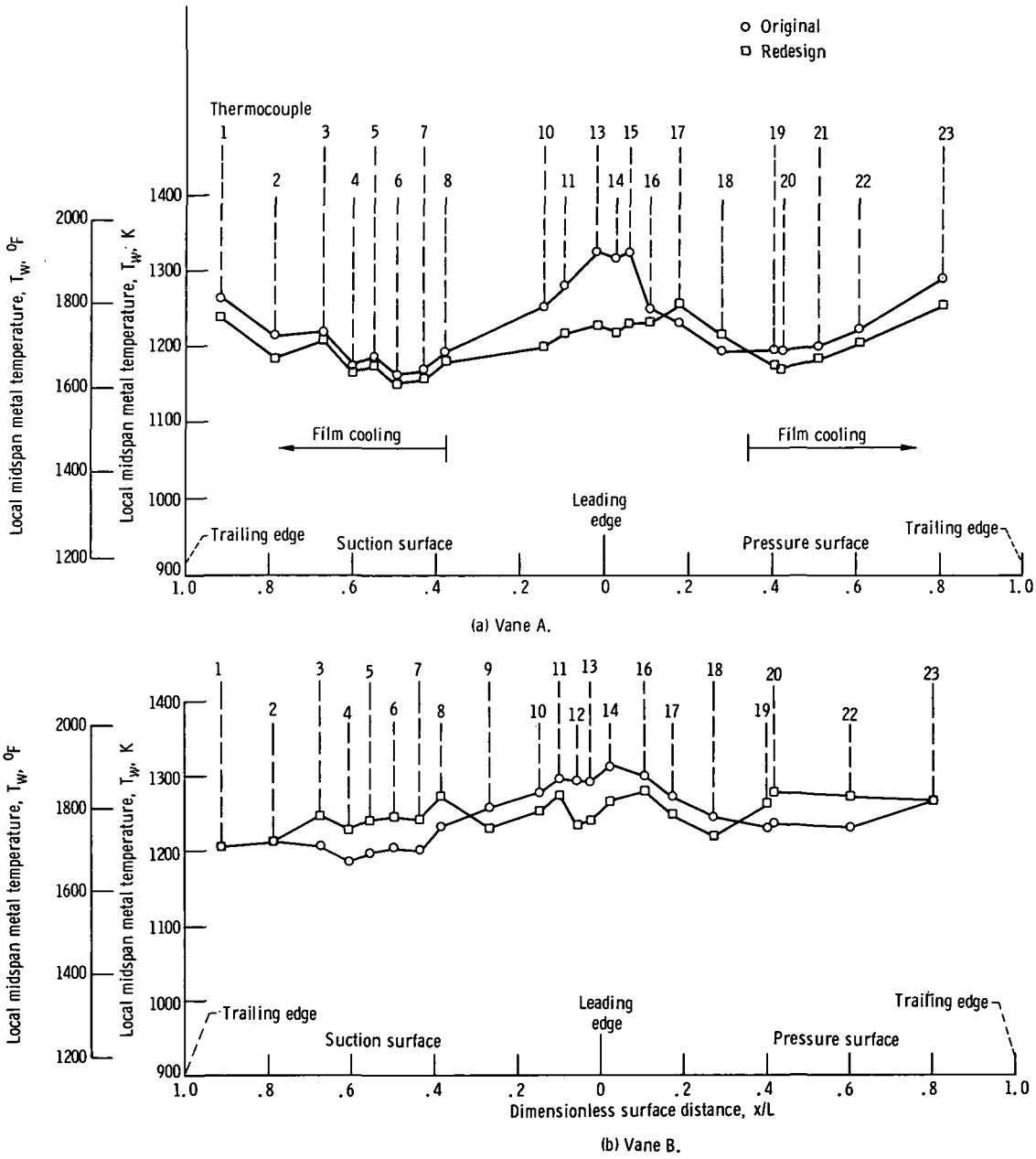

Figure 3. - Chordwise temperature distribution of vane midspan for hotspot turbine-inlet temperature of 1528 K (2290^0 F), coolant inlet temperature of 922 K (1200^0 F), and coolant- to gas-flow ratio of 0.05.

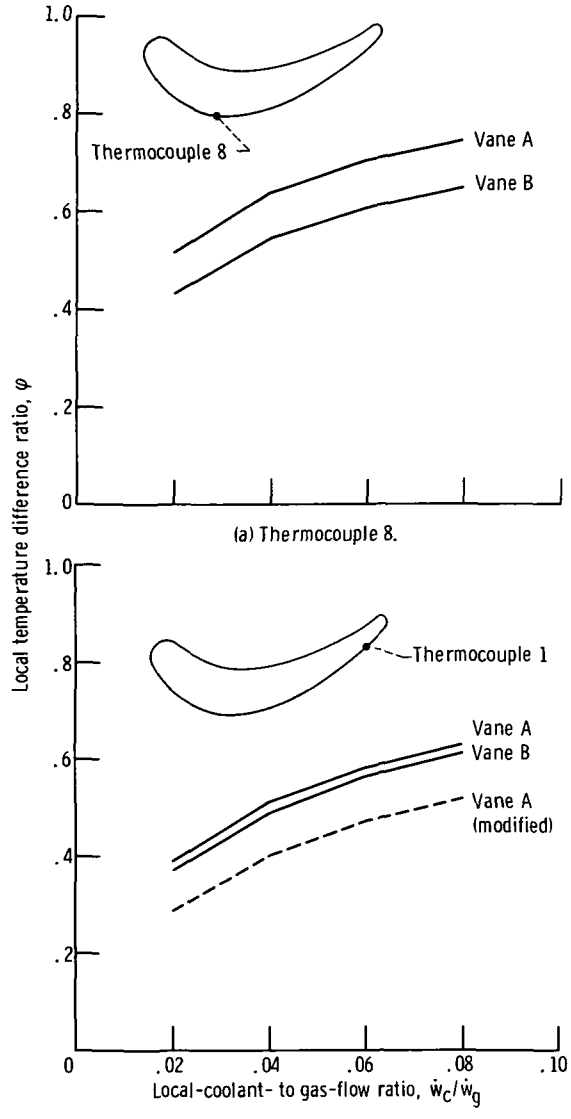

Figure 4. - Comparison of local temperature difference ratio as function of local coolant to gas flow ratio for vane A and vane B.

NATIONAL AERONAUTICS AND SPACE ADMINISTRATION
WASHINGTON, D.C. 20546

OFFICIAL BUSINESS
PENALTY FOR PRIVATE USE $300

SPECIAL FOURTH-CLASS RATE BOOK

POSTAGE AND FEES PAID
NATIONAL AERONAUTICS AND SPACE ADMINISTRATION
451

U.S.MAIL

POSTMASTER: If Undeliverable (Section 158 Postal Manual) Do Not Return

"The aeronautical and space activities of the United States shall be conducted so as to contribute . . . to the expansion of human knowledge of phenomena in the atmosphere and space. The Administration shall provide for the widest practicable and appropriate dissemination of information concerning its activities and the results thereof."

—NATIONAL AERONAUTICS AND SPACE ACT OF 1958

NASA SCIENTIFIC AND TECHNICAL PUBLICATIONS

TECHNICAL REPORTS: Scientific and technical information considered important, complete, and a lasting contribution to existing knowledge.

TECHNICAL NOTES: Information less broad in scope but nevertheless of importance as a contribution to existing knowledge.

TECHNICAL MEMORANDUMS: Information receiving limited distribution because of preliminary data, security classification, or other reasons. Also includes conference proceedings with either limited or unlimited distribution.

CONTRACTOR REPORTS: Scientific and technical information generated under a NASA contract or grant and considered an important contribution to existing knowledge.

TECHNICAL TRANSLATIONS: Information published in a foreign language considered to merit NASA distribution in English.

SPECIAL PUBLICATIONS: Information derived from or of value to NASA activities. Publications include final reports of major projects, monographs, data compilations, handbooks, sourcebooks, and special bibliographies.

TECHNOLOGY UTILIZATION PUBLICATIONS: Information on technology used by NASA that may be of particular interest in commercial and other non-aerospace applications. Publications include Tech Briefs, Technology Utilization Reports and Technology Surveys

Details on the availability of these publications may be obtained from:

SCIENTIFIC AND TECHNICAL INFORMATION OFFICE

NATIONAL AERONAUTICS AND SPACE ADMINISTRATION

Washington, D.C. 20546